Journal of Dynamic Behavior of Materials, March 2017, Volume 3, Issue 1, pp 100–109
DOI:10.1007/s40870-017-0099-1

# THE STRENGTH OF TWO HMX BASED PLASTIC BONDED EXPLOSIVES DURING ONE DIMENSIONAL SHOCK LOADING.

J.C.F. Millett[1,*], P. Taylor[1], A. Roberts[2], G. Appleby-Thomas[2].

[1]AWE, Aldermaston, Reading, RG7 4PR. United Kingdom.

[2] Centre for Defence Engineering, Cranfield University, Defence Academy of the United Kingdom, Shrivenham, Swindon, SN6 8LA. United Kingdom.

*jeremy.millett@awe.co.uk

**Abstract**. **Keywords** – plate impact; EDC32; EDC37; shear strength.

A series of experiments have been performed to probe the *mechanical* response of two HMX based plastic bonded explosives to one dimensional shock loading. Manganin stress gauges in longitudinal and lateral orientation to the loading axis have been used as the diagnostic. Results indicate that despite major differences in the binder phase and smaller differences in the HMX crystal loading and morphology, the Hugoniot and shear strengths behind the shock front are near identical. We have proposed that this is due to the HMX crystals forming a network that supports the bulk of the applied stress.

## 1. Introduction

In contrast to inert materials such as metals and alloys, ceramics or polymers, the shock response of energetic materials (explosives, propellants and pyrotechnics) are complicated by rapid chemical reactions such as deflagration and detonation. Indeed, it would be fair to say the majority of work investigating the response of these materials to shock loading has concentrated upon these very issues. The text book of Bailey and Murray [1] gives an excellent overview of these areas of research. However, energetic materials can also be considered as materials with a purely structural response to mechanical loading in common with all other non-energetics, an area that has received much less attention. Palmer and Field [2] deformed single crystals of cyclotetramethylene-tetranitramine (HMX) at quasi-static strain-rates, either via indentation using a Vickers indenter, or between glass anvils. Their results showed that whilst β-HMX was brittle, it could accommodate large strains via elastic twinning before failure. However, as load increased, non-cleavage fractures begun to develop from the crystal surface, generally near locations where twins meet that surface. It was suggested that at these points, a step could form, thus acting as a stress concentration which would facilitate fracture. It was also suggested that this would have implications for plastic bonded explosives (PBXs), since these large elastic strains in the HMX crystals could aid decohesion between them and the polymer binder. Dick and his colleagues and investigated the shock response of single crystal PETN (pentaerythritol tetranitrate) [3, 4] and HMX [5, 6]. In the case of PETN, it was observed that the <110> orientation had the highest likelihood of reaction, then <001>, <101> and finally <100>. This was correlated with the ease of deformation via

dislocation motion, thus a direction where ease of dislocation motion was observed, was also observed to have a high detonation threshold. A later study on the response of single crystal HMX [6] also showed a dependence of elastic precursor amplitude on crystalline orientation, with the {010} orientation having a higher precursor amplitude than either the {110}, or {011} orientations, which were near identical. In that work, it was suggested that for the {110} planes, one slip and twin system, and the fracture plane were all oriented approximately 45° to the impact axis, whilst in the {011} planes, the same slip and twin systems were available, but the fracture plane was not. Therefore for these two orientations, plasticity, be it dependent on dislocation motion or twin formation was the preferred deformation mechanism. For the {010} orientation, the slip and twin systems were both at 90° to the impact plane, thus rendering them unavailable, thus leaving only fracture as a viable deformation response. Finally, Hooks *et al*. [7] performed a similar set of experiments on cyclotrimethylene trinitramine (RDX). Although no differences in precursor amplitude were noted between orientations {210}, {111} and {100}, significant differences were observed in the shock profiles. In the {210} orientation, the profiles showed a conventional separation between the elastic and inelastic components of the shock front, whilst in the {111} orientation, the velocities of the two components were near identical, with only a slight inflexion indicating separation in thicker specimens. The {100} showed a stepped like nature below the elastic limit. It was noted that in this orientation, the angles of the deformation planes were 90°, hence plastic deformation would not likely occur. It was therefore suggested that these steps my be the result of cracking, possible prior to shock loading, either during target assembly or anisotropic thermal expansion due to heating from the laser used as the diagnostic.

Most energetic materials are used as part of a composite system, with energetic crystals embedded in either an inert or energetic binder, creating PBXs. As a consequence, whilst a body of work has been performed to probe their mechanical response at quasi-static and intermediate strain-rates (see references [8-10]) and under conditions of Taylor impact [11], equivalent studies under one-dimensional shock loading is much less prevalent. The inert response (in terms of particle velocity – $u_p$ and shock velocity – $U_S$) has been studied either as part of a wider study on the equation of state [12-15], or in terms of their purely inert response [16, 17]. However, reports on the mechanical properties themselves (for example Hugoniot Elastic Limit – HEL, spall strength or shear strength) are extremely scarce. Martinez *et al*. [18], used ytterbium gauges to measure the longitudinal and lateral components of stress in an effort to determine the shear strength behind the shock front. Dick [19] managed to observe the yield under one dimensional strain in PBX9501 (HMX based) at a stress of *ca*. 145 MPa, whilst Burns *et al*. [14] determined the HEL in EDC32 at a level of 220 MPa. A feature of many materials concerns the relationship between the imposed shock stress ($\sigma$) and the strain-rate in the shock front ($\dot{\varepsilon}$). Swegle and Grady [20] noted that that the two were related through the fourth power, of the form,

$$\sigma = A\dot{\varepsilon}^4, \qquad (1)$$

where A is a scaling factor. Although this analysis was intitially only applied to metals, in a later publication, Grady [21] was also able to apply it to a number of other materials, including particulate based composites such as alumina-epoxy, and the HMX based PBX

PBX9501. In a very recent paper, Whiteman *et al.* [22] were able to provide a qualitative correlation (in metals) between the constant $A$ and the ease of dislocation motion and multiplication. In principle, this relation should yield information concerning the likely deformation mechanisms, but given that to our knowledge, PBX9501 is the only PBX to have undergone this analysis, no further comment can be made at this time.

As PBXs can be considered as composites with a high loading of hard particles in a softer matrix, it is useful to consider similar materials using an inert particulate such as sugar [16], soda-lime glass beads [23] or alumina [24, 25]. In general, the relationship between shock and particle velocity can be expressed in simple linear terms in the form,

$$U_S = c_0 + Su_p \qquad 2.$$

where $c_0$ and $S$ are empirical constants, although in some materials, notably metals, these have been related to the bulk sound speed and first derivative of bulk modulus with pressure [26]. In a group of RDX - HTPB (hydroxy terminated polybutadiene) based PBXs, Bourne and Milne [13] and Milne *et al*. [17] showed that the Hugoniot was non-linear at low particle velocities, even though the Hugoniot of HTPB itself was shown to be linear [27, 28]. Similar effects were noted in a composite consisting of soda-lime glass beads in HTPB [23] and more complex epoxy based composites such as epoxy-aluminium-$MnO_2$ [29]. This led to the suggestion that this change in slope of the $U_S$-$u_p$ curve was due to the elastic – inelastic transition the 'crystalline' phase and has also been applied to non-linear behaviour observed in some semi-crystalline polymers [30]. However, this has not been observed in HMX based PBXs such as EDC32 [14], EDC37

[12] and PBX 9501 [31] or the triamino-trinitrobenzene based material PBX9502 [32]. A number of possible explanations occur, including very high explosive loading (EDC37 – 91 wt%, PBX9501 and PBX9502 – both 95 wt%) compared to the RDX based materials discussed above – 88wt% [13] or similarities in the acoustic and shock response of the explosive crystals and organic binder as in EDC32 [14], even though the explosive loading is lower (85 wt%). Beyond this, little attention has been given to the mechanical response of this class of material to shock loading. In a previous report, it was observed that although the hydrodynamic response of glass-HTPB composites was insensitive to the size of glass particles (the balance of phases present being otherwise equal), the Hugoniot stress was strongly influenced by particle size, with a coarser material being the stronger [23]. In work, it was suggested that the presence of coarser glass particles hindered the materials' ability to flow, forcing deformation to occur between those larger particles, whilst the finer material had more ability to flow as a whole. Similar observations were noted in PBX stimulant materials, using different sizes of inert particles.

## 2. Materials

EDC32 is a plastic bonded explosive, consisting of (by weight) 85% HMX with the remaining 15% Viton-A (a co-polymer of vinylidene difluoride and hexafluoropropylene – manufactured by DuPont) [14]. In terms of balance of phases, it is identical to the US composition LX-04, although there are differences in the size and distribution of HMX crystals. Both materials have approximately 66wt% of crystals below 50 μm; however, whilst in EDC32 the majority (<99wt%) of crystals are below 125 μm, in LX-04 about 4wt% of crystals have a size range 150 – 300 μm. Whilst this is unlikely to effect the

equation of state (EoS), it will almost certainly effect the shock induced mechanical properties, as has already been seen in soda-lime glass – HTPB [23] and sugar – HTPB composites [16]. The material generally has a porosity of *ca*. 1.5%. EDC37 is a pressed HMX based PBX, consisting of 91wt% HMX in a weak bi-modal distribution of crystals with the majority in the region of 100 µm and the remainder below 10 µm. The binder consists of 8 wt% K10 liquid plasticizer and 1 wt% nitrocellulose. The material is pressed to greater than 99% of theoretical maximum density, with no noticeable porosity. The basic shock and acoustic properties are summarized in Figure 1 and Table 1.

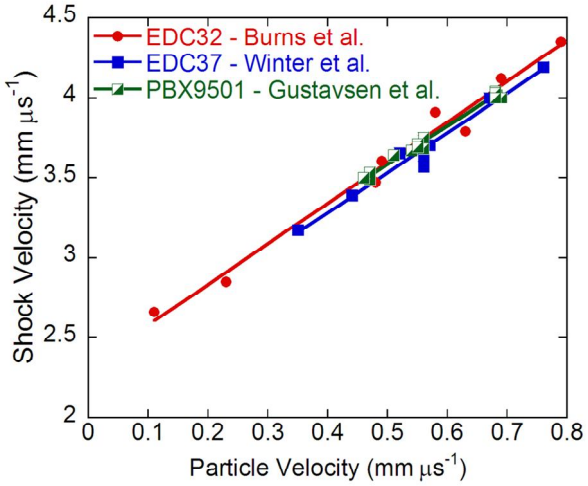


Figure 1. Inert shock velocity versus particle velocity for three HMX based PBXs – EDC32 [14], EDC37 [12] and PBX9501 [31].

We have also included data from the US composition, PBX9501. This is an HMX based material, consisting of a bi-modal particle distribution at 10 and 200 µm, although this can extend up to 500 µm. The binder is a 50/50 mixture of estane (a polyurethane elastomer)

and a nitrated plasticser. The total HMX loading is 95wt%, and the final material has 2 to 3% porosity.

Table 1. Materials and shock properties of HMX based PBXs. Also included are the equivalent properties for pure HMX [33, 34] and Viton-B [35, 36].

| | $\rho_0$, g cm$^{-3}$ | $c_0$, mm μs$^{-1}$ | $S$ | $c_L$, mm μs$^{-1}$ | $c_S$, mm μs$^{-1}$ | $c_B$, mm μs$^{-1}$ | $\nu$ |
|---|---|---|---|---|---|---|---|
| EDC32 | 1.86 | 2.32 | 2.54 | 2.78 | 1.41 | 2.25 | 0.327 |
| EDC37 | 1.84 | 2.28 | 2.50 | 2.66 | 1.09 | 2.34 | 0.399 |
| PBX9501 | 1.83 | 2.38 | 2.41 | 2.97 | 1.39 | 2.50 | 0.360 |
| HMX | 1.90 | 2.74 | 2.60 | 2.79 | 1.40 | 2.27 | 0.333 |
| Viton-B | 1.96 | 1.88 | 2.37 | 1.71 | 0.71 | 1.50 | 0.396 |

We have included the acoustic and shock properties of pure, pressed HMX as a comparison to the PBX compositions. As far as we are aware, neither the acoustic or shock response of Viton-A is not available within the open literature. Therefore we have included the data of the chemically similar Viton-B [35, 36]. Although it is unlikely that the properties of these two polymers will be identical, past experience with highly fluorinated polymers [30, 37] suggests that an understanding of these materials can assist in the analysis of the shock response of EDC32.

## 1 Experimental

Plate impact experiments were performed using the 6 m long, 51 mm bore, single stage gas launcher, based at Cranfield University [38]. Longitudinal stresses in the range 0.64-4.13 GPa were induced by the impact of 5 mm thick flyer plates of either Dural

(aluminium alloy 6082-T6) or copper in the velocity range 188 - 547 m $s^{-1}$. The main purpose of these experiments was to measure the shock induced shear strength behind the shock front. As such, manganin stress gauges were mounted both longitudinally and orthogonally to the impact axis. 10 mm thick, 60 mm diameter disks of EDC32 and 37 were sectioned in half and a manganin stress gauge (MicroMeasurements type J2M-SS-580SF-025) was introduced 2 mm from the front surface. The target was reassembled using a compatible polyurethane adhesive. The placement of this gauge renders it sensitive to the lateral component of stress ($\sigma_y$). Gauge data were reduced from the raw voltage-time traces using the methods of Rosenberg *et al*. [39] After, the front surface was lapped back, and then attached to a 1 mm thick coverplate of either Dural or copper, matched to the material of the flyer plate. A second manganin gauge (MicroMeasurements type LM-SS-025CH-048) was placed between the coverplate and the explosive, such that it was sensitive to the longitudinal component of stress ($\sigma_x$). Gauge calibrations were according to Rosenberg *et al*. [40] In this way, not only would the impact stress be directly measured, but through impedance matching, the particle velocity could also be determined, and hence the Hugoniot over the entire impact range of these experiments be obtained. A representative diagram of the target assembly is shown in figure 2a. whilst a photograph of a similar target assembly (in this case made from PCTFE [41] as a test run for the present investigation) in situ within the specimen chamber of the gun is shown in figure 2b. Note that both gauges are connected to the wider gauge circuitry via a mechanical dry joint rather than soldered to avoid equipment at elevated temperatures coming into possible contact with the explosive targets.

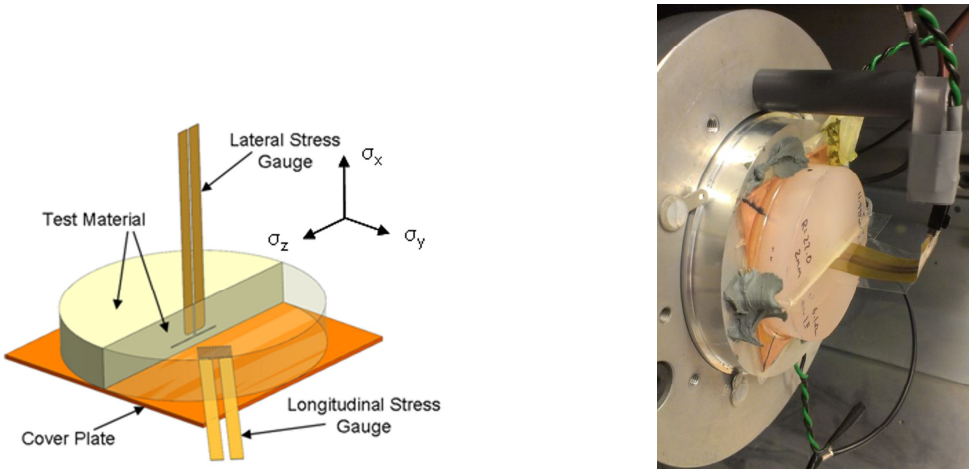


a. Schematic b. Target assembly in situ

Figure 2. Schematic diagram and photograph of a typical target assembly in place in the target chamber.

The Hugoniot (or longitudinal) stress can be separated into hydrostatic ($P$) and shear ($\tau$) components, thus,

$$\sigma_x = P + \frac{4}{3}\tau \,. \tag{3}$$

If it is then assumed that the material is behaving isotropically (not unreasonable given that both PBXs consist of HMX crystals distributed nominally randomly in a binder), then the hydrostatic pressure can be expressed as an average of the orthogonal components of stress,

$$P = \frac{\sigma_x + \sigma_y + \sigma_z}{3} \tag{4}$$

and that under conditions of one dimensional strain, the applied stress is cylindrically symmetrical around the x-axis, combining equations 3 and 4 yields an expression for $\tau$ (the shear strength) in terms of the longitudinal and lateral stresses,

$$2\tau = \sigma_x - \sigma_y . \qquad (5)$$

## 2 Results

Representative gauge traces (in both longitudinal and lateral orientation) from both PBX compositions are presented in figure 3.

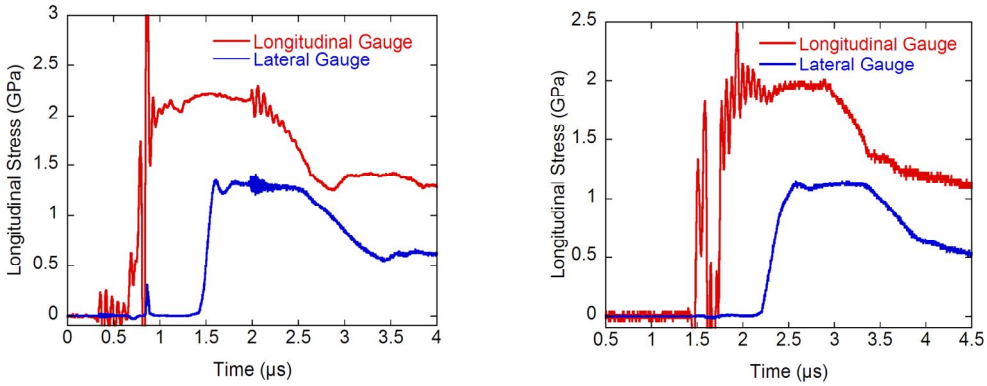


a. EDC32, 338 m $s^{-1}$. b. EDC37, 372 m $s^{-1}$.

Figure 3. Longitudinal and lateral stress gauge traces from shock loaded PBXs, impacted with 5 mm Dural flyers.

Observe that there appears to be a degree of superimposed noise, particularly on the longitudinal gauge traces. Such behaviour has been noted before, for example in pressed sugar and sugar based composites [16, 42] as well as HMX based materials, although in

this case, the noise was not as prevalent. In those works, it was proposed that this be due to fracto-emission of the HMX particles causing excess electrical noise. Note that it is more noticeable on the longitudinal gauges, which have a much greater active area than the lateral gauges (see figure 1). Finally, it can be seen that although excess electrical noise is present on the longitudinal stress traces of both materials, it is much more significant in EDC37 than EDC32. This may simply be due to the fact that EDC32 has a lower HMX loading than EDC37 and thus the lower degree of fracto-emission in EDC32 may just be due to the fact that fewer HMX crystals are available for fracture. A more detailed examination of the lateral stress response in these materials is shown in figure 4.

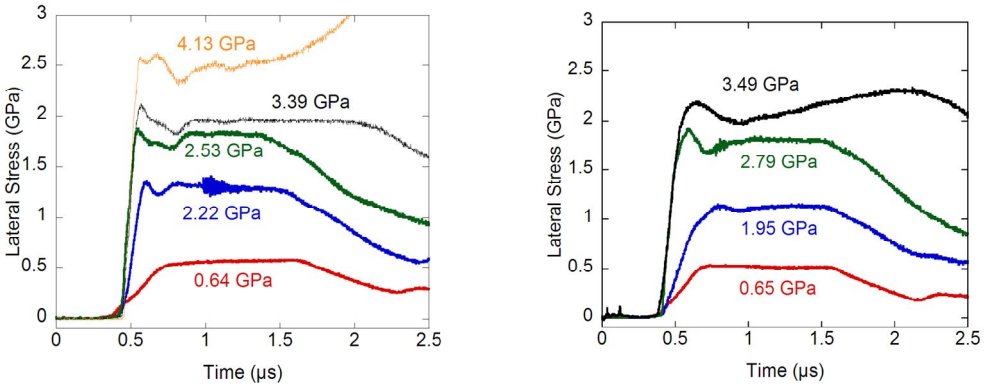


a. EDC32 b. EDC37

Figure 4. Lateral stress traces from EDC32 and EDC37. The gauges were 2 mm from the front surface. Each trace is labelled with the impact stress.

There are more complex features in both sets of traces that need to be addressed. Firstly, the rise times in both materials appear to decrease as shock amplitude increases,

indicating a stiffening as stress increases. Also notice that the traces in EDC37 have a more rounded nature than in EDC32, possibly due to the differing nature of the binder phase (near liquid in EDC37 compared to a more rigid fluorocarbon in EDC32). Finally, observe that in both materials, as stress amplitude increase, the traces become increasingly complex, to the point at the highest amplitude lateral stress starts to increase behind the shock front. We believe that the most likely cause for this is that the onset of reaction is occurring, thus affecting the output of the gauges.

The longitudinal stress data generated from the gauge data presented in figure 3 has been used via the technique of impedance matching to calculate the corresponding particle velocities, hence allowing us to present the Hugoniots of EDC32 and EDC 37 in figure 5.

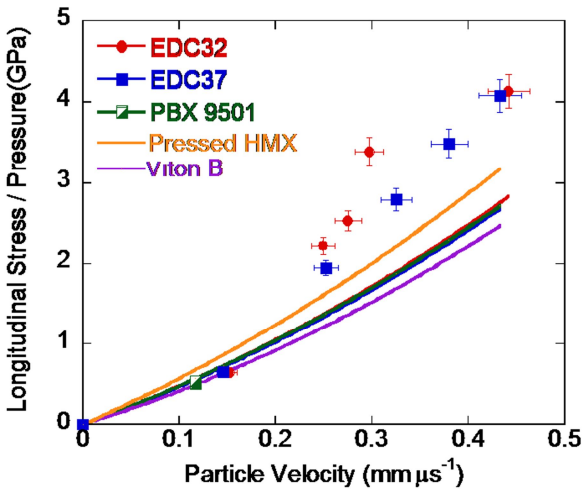


Figure 5. The Hugoniot (in stress – particle velocity space) for EDC32 and 37. Also included is a single point for PBX 9501 [18]. The curve fits are the hydrodynamic response generated from equation 4, and the data presented in Table 1. We have also included the hydrodynamic response for pure HMX [33] and Viton B [35].

We have also included a couple of equivalent data points from the work of Martinez *et al*. [18] from PBX 9501. In addition, we have also fitted the data to the hydrodynamic response ($P_{HD}$), using the appropriate data from table 1 via,

$$P_{HD} = \rho_0 (c_0 + S u_p) u_p . \qquad (4)$$

It can be seen that as particle velocity increases, the difference between the measured stresses and the hydrodynamic pressure also increases. As can be seen from equation 2, this suggests that the shear strength behind the shock front (for the experimental range in this investigation) is increasing with increasing impact stress, although it should be pointed out that the hydrostatic ($P$) and hydrodynamic ($P_{HD}$) pressures are not precisely the same. Note that both the measured stresses (allowing for a degree of scatter) for EDC32 and EDC37 are near identical, as is the hydrodynamic response (both in terms of $U_S$-$u_p$ and $P_{HD}$-$u_p$) for EDC32, 37 and PBX 9501. This can be taken as a first indication that the mechanical response to shock loading in HMX based PBXs are largely dominated by the presence of the HMX crystals.

This issue is explored further, using the shear strengths calculated using equation 4 and the gauge data presented in figures 3 and 4 and their variation with longitudinal stress is shown in figure 6 The straight line fits assume a purely elastic response, according to,

$$2\tau = \frac{1-2\upsilon}{1-\upsilon}\sigma_x, \qquad (5)$$

where $v$ is the Poisson's ratio.

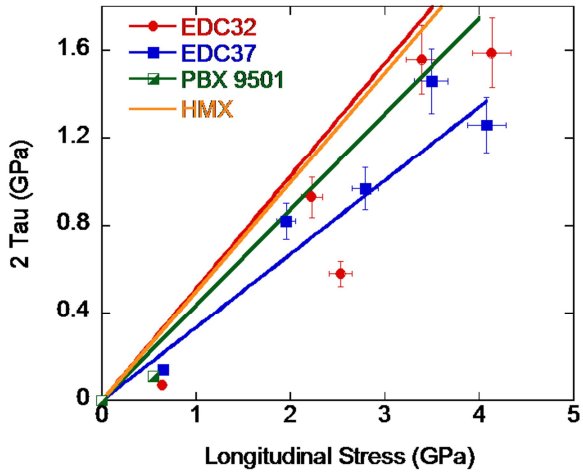


Figure 6. Shear strength versus longitudinal strength for HMX based PBXs. The straight lines are elastic fits according to equation 5.

In both compositions, shear strength appears to increase with longitudinal stress, as was hypothesised when comparing the Hugoniot to the hydrodynamic response. Given the scatter within the data it is difficult to make any other judgement than that the shear strengths of these two materials are near identical. The shear strength calculated by Martinez *et al*. [18] also seems to agree with our own data, but given that there is only one data point available and that it was made at a very low stress, it would be unwise to draw too definitive a conclusion.

## 3 Discussion

Like all solid materials, PBXs will have a mechanical response to shock loading that is governed by factors such as microstructure, strain-rate and temperature. Unlike inert solids, this response is complicated by the onset of reaction (deflagration and detonation) which is where the majority of work has concentrated. As a consequence, we have taken the opportunity to study the purely mechanical response of two of these materials (the HMX based PBXs EDC32 and EDC37), using manganin stress gauges in longitudinal and lateral orientation to the shock loading axis. This technique has been used previously on metals [43, 44], ceramics and silicate glasses [45, 46], polymers [47, 48] and particulate composites [24]. The primary goal of this investigation is to determine the shear strength of these materials, both as a function of imposed shock stress and its variation with time behind the shock front. Although the input from both longitudinally and laterally orientated gauges is needed to determine the shear strength (equation 4), the individual gauge traces themselves still yield a great deal of information about the response of a material. Starting with the longitudinal gauges, it can be seen from figure 3 that the traces from both materials have a level of superimposed noise. Such behaviour has been noted previously, both in surrogate materials (pure and as polymer bonded composites) and to a lesser extent HMX, and HMX and RDX based composites [16, 42]. Both reports noted that this behaviour was more prevalent in the materials with a larger particle size, leading to the suggestion that this noise was due to fracture in the larger particles causing fracto-emission to create electrical noise that is picked up by the gauges. Observe that this is more significant on the longitudinal gauge traces than the lateral gauges. The longitudinal gauges used on this investigation are of dimension *ca*. 4 mm x 5 mm square, giving an

active area of 20 $mm^2$. In contrast, the lateral stress gauges have an active width of 15 mm, but are only 240 μm wide, thus giving an active area of just 3.75 $mm^2$. Thus the longitudinal gauges have a much greater area, and hence greater efficiency to pick up excess electrical noise. A final point to draw from the superimposed noise on the gauge traces is that it is greater in EDC37 than EDC32. Whilst the HMX particle sizes in both materials are not significantly different, the overall loading (in weight%) is, with EDC37 at 91%, compared to EDC32 at 85%. Therefore EDC37 is likely to experience more fracto-emission, and thus more noise on the gauge trace, simply due to the fact that there is more HMX present than in EDC32.

Aside from the fracto-emission on the longitudinal gauge traces giving an indication of the operative deformation mechanisms, their main purpose was to determine the impact stress, and through impedance matching techniques, the corresponding particle velocities and hence the Hugoniot of the materials concerned. As the gauge was supported on the front of the explosive target with a 1 mm thick plate of material matched to that of the flyer plate, the traces themselves would (apart from the imposed noise) be expected to be relatively featureless given that the shock front at that point has only travelled through 1 mm of either Dural or copper. The Hugoniots of both EDC32 and 37 have been plotted in figure 5, and we have also included the calculated hydrodynamic pressures calculated from equation 4. As a comparison, we have also included the response of the similar PBX9501 [31], pressed HMX [33] and Viton-B [35]. A number of features are immediately apparent from this figure. Firstly, the measured Hugoniot points of EDC32 and 37 lie (at higher particle velocities) significantly above the calculated response. From equation 2, this is a strong indication that these materials have a significant shear strength under shock loading

conditions. Also note that the hydrodynamic response, both in terms of $U_S$-$u_p$ (figure 1 and Table 1) and the hydrodynamic pressure (figure 5) are effectively identical, as are the Hugoniot stresses, although in this case, there is a degree of scatter. This is a first suggestion that the shock induced shear strengths are near identical for both materials, even though the HMX loadings are somewhat different (85wt% for EDC32 and 91wt% for EDC37). This also suggests that at these compositions, the strength of these materials is dominated by the presence of the HMX crystals themselves with the binder phase only having a minimal contribution.

Although it has been possible to infer some of the mechanical responses to shock loading from the longitudinal gauge traces alone, analysis of the lateral gauge traces (in combination with the longitudinal stress response) is more revealing. The basic features shown by the lateral stress histories (figure 4) are an initial sharp rise in stress to a near constant stress level, followed by a decrease in stress as releases from the rear of the flyer enters the gauge location. However, the actual response shows behaviour to be a little more complex. In all but the lowest amplitude traces, there appears to be a small drop in lateral stress amplitude, occurring for approximately 100 to 300 ns, before rising back to a constant stress. Such behaviour has been noted in other materials, for example epoxy-alumina composites [25] where this was attributed to the fast rising nature of the shock exceeding the response time of the gauge, thus causing a small degree of ringing in the signal. However, the length of this part of the signal in the PBX traces suggests that these features may indeed be mechanical, and thus require explanation. An interesting possibility comes from the work of Petel and Higgins [49], who examined the shock response of suspensions of silicon carbide powder in ethylene glycol. They demonstrated that whilst at

low shock stresses, the response was dominated by the compressibility of ethylene glycol matrix, as stress increased, stress linking between silicon carbide particles became increasingly dominant, causing a shift in $U_S$-$u_p$ behaviour to a stiffer response. The use of lateral stress gauges also showed that whilst pure ethylene glycol behaved as a typical liquid (*i.e*. longitudinal and lateral stresses were identical), mixtures with silicon carbide contents from 66.8 to 77.3wt% could support considerable shear stresses (around 0.5 GPa). The particulate loading in the PBXs in this investigation are much higher (85 and 91wt%), and hence the establishment of particulate force chains is likely to be much faster. We therefore believe that this initial part of the signal is due to the complex rearrangement of HMX particles before a stable network is established. However, only in EDC37 can the binder be considered a liquid, whilst the more rigid Viton-A binder in EDC32 will also work against particle bridging. This can also be seen in the rising part of the lateral stress traces. It is clear that these are much faster in EDC32, again due to the more rigid nature of the Viton-A binder. The near liquid nature of the K10/nitrocellulose binder in EDC37 is more likely to allow some degree of particle movement during the initial stages of shock loading, leading to a more dispersive shock, even though the HMX loading is higher. The final observation worthy of note from the lateral stress histories, is at the highest amplitudes shown, where lateral stress rises approximately 1 μs after the shock arrival at the gauge. We believe that this is most likely due to the build up to reaction. Reaction in EDC32 and 37 has been observed at stresses as low as 3.33 GPa [14] and 2.69 GPa [12] respectively. The fact that we don't see at least the beginnings of reaction until the very highest amplitudes suggests that releases from the rear of the flyer plates are entering the gauge locations before reaction can begin, in effect quenching reaction before it can begin.

The shear strengths, generated from knowledge of the longitudinal and lateral stress gauge data shown in figure 6 indicates, after taking the degree of scatter into account that there is little if any difference in shear strength between EDC32 and 37. An additional shear strength point from PBX9501 [18] also shows agreement with our own data, but given that it is just one point at a very low stress amplitude, any similarities should at this point be taken with caution. However, the similarities in shear strength between EDC32 and 37 shown here are in agreement with the observations made previously concerning the Hugoniot, and lend support to our hypothesis that the mechanical response of highly loaded HMX based PBXs is controlled by the transmission of stress through the HMX particle network, with the binder phase having only a small contribution. A number of straight lines have also been fitted to this set of data, assuming that the materials are behaving purely elastically (equation 6) using the appropriate values of Poisson's ratio from table 1. The gradients of these lines are controlled by the Poisson's ratio of the material in question, ranging from 0.399 for EDC37 to 0.327 for the more rigid EDC32, with pure, polycrystalline HMX at 0.333. Looking at how the measured shear strengths lie in comparison with the calculated elastic strengths, it would appear that at least EDC37 is behaving elastically. Given the liquid like nature of the binder phase in this material, this would seem extremely unlikely. However, if our previous supposition is correct, namely that the strength of highly loaded HMX based PBXs is controlled almost exclusively by the HMX itself, the situation becomes clearer. Therefore, instead of considering the elastic response of the particular PBX composition, we should in fact be looking at the elastic response of pure HMX. In this case, all data lies below this line, indicating that there is inelastic deformation (dislocation based plasticity, twinning and fracture) in the HMX

crystals. Although Dick *et al*. [6] measured HELs in single crystals at 0.4 GPa for the {110} and {011} orientations and 0.8 GPa for the {010} orientation, there appears to be no equivalent data for polycrystalline HMX. However, Burns *et al*. [14] did manage to measure the HEL in EDC32, quoting a value of 220 MPa, whilst Dick obtained values of the HEL in PBX9501 of 145 MPa [19]. At the time of writing, neither set of authors presented a value of the shear strength, but from the data in table 1, we can obtain a value of $2\tau$=110 MPa and 63 MPa respectively.. This would be consistent with the observation that our own measurements in both EDC32 and 37 are above both the yield points in the PBXs themselves and the HMX crystals as well. Although the available data within the literature is extremely limited, it would suggest that the initial yield in PBXs is controlled by the binder. Note that EDC32 has a Viton-A binder which is likely to be stronger than the estane-nitroplasticiser binder used in PBX9501.

One final point worthy of consideration is the similarity in the mechanical response of these materials, given that there are differences in microstructure, binder phase and HMX content. From previous experience in inert stimulant compositions [16, 23], significant changes in strength were observed, due to changes in particle size, even when the balance of phases was kept constant. However, it should be pointed out that in those works, changes in particle size were of the order of an order of magnitude (16 and 160 μm in the sugar based simulants [16] and 30 and 300 μm in the glass-HTPB composites [23]). In the case of the PBXs examined here, EDC32 has a majority of HMX crystals of size 125 μm or less, whilst EDC37 has a bimodal distribution of HMX crystals, the majority of which are approximately 100 μm. Therefore, although the size and distribution of HMX are different, we do not believe that those differences are enough to cause noticeable

differences in shear strength above the yield point. Even with PBX9501, where the particle size is quoted as a bimodal distribution of 10 and 200 μm, it is likely that there is not enough difference to cause noticeable changes in the shear strength, although as yet, this still needs experimental confirmation.

## 5 Conclusions

A series of plate impact experiments have been performed on the plastic bonded explosives, EDC32 and 37, designed to probe their purely mechanical response to shock loading. The use of manganin stress gauges, orientated both longitudinally and laterally to the loading axis have revealed a number of features;

- The Hugoniot stress, and thus the offset from the hydrodynamic pressure is near identical in both materials.
- Both materials show evidence of electrical pickup on the longitudinal gauges; this is more prevalent in EDC37.
- The shear strength determined from longitudinal and laterally mounted stress gauges is near identical in both materials
- EDC37 shows a slower rise time from the lateral stress histories compared to EDC32.

Therefore, in combination with yielding information from the literature, we propose that whilst yield itself is controlled by a number of factors, including nature of the binder phase, size and distribution and balance of the HMX crystals, at high HMX loadings within the microstructure, the shear strength appears similar, if not identical between the two

materials studied here. We have proposed that this is due to the majority of the applied stress being supported by the network of HMX particles.

**Acknowledgments**

From AWE, we would like to thank Malcolm Burns, Mike Goff, James Ferguson, Caroline Handley and Nick Whitworth for useful discussions during the writing of this paper. We would also like to thank Chris Stennet and Dave Wood of Cranfield University for their help in the experimental programme.



**References**

[1] Bailey A and Murray SG (1989) Explosives,Propellants and Pyrotechnics Brassey's London

[2] Palmer SJP and Field JE (1982) The deformation and fracture of beta-HMX. Proc. R. Soc. Lond. A. Math. Phys. Sci 383:399-407

[3] Dick JJ, Mulford RN, Spencer WJ, Pettit DR, Garcia E and Shaw DC (1991) Shock response of pentaerythritol tetranitrate single crystals. J. Appl. Phys. 70:3572-3587

[4] Dick JJ and Ritchie JP (1994) The crystal orientation dependence of the elsatic precursor shock strength in the PETN molecular explosive and the modeling of the steric hinderance to shear by molecular mechanics. J. Phys IV (DYMAT) Colloque C8:393-398

[5] Dick JJ, Hooks DE, Menikoff R and Martinez AR (2004) Elastic-plastic wave profiles in cylcotetramethylene tetranitramine crystals. J. Appl. Phys. 96:374-379

[6] Dick JJ and Martinez AR (2002) Elastic precursor decay in HMX explosive crystals. In: M. D. Furnish, N. N. Thadhani and Y. Horie (ed) Shock Compression of Condensed Matter - 2001. AIP Press, Melville, NY, pp 817-820

[7] Hooks DE, Ramos KJ and Martinez AR (2006) Elastic-plastic shock wave profiles in orientated single crystals of cyclotrimethylene trinitramine (RDX) at 2.25 GPa. J. Appl. Phys. 100:024908

[8] Idar D, Thompson DG, Gray GT, Blumenthal WR, C.M. Cady, Peterson PD, Roemer EL, Wright W and Jacque BL (2002) Influence of polymer molecular weight, temperature and strain-rate on the mechanical properties of PBX 9501. In: M. D. Furnish, N. N. Thadhani and Y. Horie (ed) Shock Compression of Condensed Matter - 2001. AIP Press, Melville, NY, pp 821-824

[9] Mas EM, Clements BE, Blumenthal WR, Cady CM and Gray GT (2002) Applying micro-mechanics to finite element simulations of split Hopkinson pressure bar experiments on high explosives. In: M. D. Furnish, N. N. Thadhani and Y. Horie (ed) Shock Compression of Condensed Matter - 2001. AIP Press, Melville, NY, pp 539-542

[10] Govier RK, Gray GT and Blumenthal WR (2008) Comparison of the influence of temperature on the high-strain-rate mechanical repsonses of PBX 9501 and EDC37. Mat. Trans A 39:535-538

[11] Clements BE, Thompson DG, Luscher DJ, DeLuca R and Brown GW (2012) Taylor impact tests and simulations of plastic bonded explosives. In: M. L. Elert, W. T. Buttler, J. P. Borg, J. L. Jordan and T. J. Vogler (ed) Shock Compression of Condensed Matter - 2011. AIP Press, Melville, NY, pp 661-664

[12] Winter RE, Sorber SS, Salisbury DA, Taylor P, Gustavsen R, Sheffield S and Alcon R (2006) Experimental study of the shock response of an HMX-based explosive. Shock Waves 15:89-101

[13] Bourne NK and Milne AM (2004) Shock to detonation transition in a plastic bonded explosive. J. Appl. Phys. 95:2379-2385

[14] Burns MJ, Gustavsen RL and Bartram BD (2012) One-dimensional plate impact experiments on the cyclotetramethylene tetranitramine (HMX) explosive EDC32. J. Appl. Phys. 112:064910

[15] Goveas SG, Millett JCF, Bourne NK and Knapp I (2006) One-dimensional shock and detonation characterization of ultrafine hexanitrostibilene. In: M. D. Furnish (ed) Shock Compression of Condensed Matter - 2005. AIP Press, Melville, NY, pp 1065-1068

[16] Millett JCF and Bourne NK (2004) The shock Hugoniot of a plastic bonded explosive and inert simulants. J. Phys. D. Applied Physics 37:2613-2617

[17] Milne A, Longbottom A, Bourne N and Millett J (2007) On the unreacted Hugoniots of three plastic bonded explosives. Propellants, Explosives, Pyrotechnics 32:68-72

[18] Martinez AR, Hooks DE and Dick JJ (2004) Longitudinal and lateral ytterbium gauge measurements in PBX 9501. In: M. D. Furnish, Y. M. Gupta and J. W. Forbes (ed) Shock Compression of Condensed Matter - 2003. AIP Press, Melville, NY, pp 792-795

[19] Dick JJ (2000) Stress-strain response of PBX 9501 below 1 Gigapascal from embedded magnetic gauge data using Lagrangian analysis. In: M. D. Furnish, L. C. Chhabildas and R. S. Hixson (ed) Shock Compression of Condensed Matter - 1999. AIP Press, Melville, NY, pp 683-686

[20] Swegle JW and Grady DE (1985) Shock viscosity and the prediction of shock wave rise times. J. Appl. Phys. 58:692-701

[21] Grady DE (2010) Structured shock waves and the fourth-power law. J. Appl. Phys. 107:013506

[22] Whiteman G, Keightley PT and Millett JCF (2016) The Behaviour of 2169 Steel Under Uniaxial Stress and Uniaxial Strain Loading. Journal of the Dynamic Behavior of Materials 2:337-346

[23] Millett JCF, Bourne NK, Akhavan J and Milne AM (2005) The response of soda-lime glass - hydroxyterminated polybutadiene composites to shock loading. J. Appl. Phys. 97:043524

[24] Millett JCF, Bourne NK and D.Deas (2005) The equation of state of two alumina-filled epoxy resins. J. Phys. D. Applied Physics 38:930-934

[25] Millett JCF, Deas D, Bourne NK and Montgomery ST (2007) The deviatoric response of an alumina filled epoxy composite during shock loading. J. Appl. Phys. 102:063518

[26] Davison L and Graham RA (1979) Shock Compression of Solids. Physics Reports 55:255-379

[27] Millett JCF, Bourne NK and Akhavan J (2004) The response of hydroxy-terminated polybutadiene to one-dimensional shock loading. J. Appl. Phys. 95:4722-4727

[28] Jordan JL, Montaigne D, Gould P, Neel C, Sunny G and Molek C (2016) High Strain Rate and Shock Properties of Hydroxyl-Terminated Polybutadiene (HTPB) with Varying Amounts of Plasticizer. J. Dynamic Behavior Mater. 2:91-100

[29] Jordan JL, Dattelbaum DM, Sutherland G, Richards DW, Sheffield SA and Dick RD (2010) Shock equation of state of a multi-phase epoxy-based composite ( Al – MnO 2 - epoxy). J. Appl. Phys. 107:103528

[30] Bourne NK, Millett JCF, Brown EN and Gray GT (2007) Effect of halogenation on the shock properties of semicrystalline thermoplastics. J. Appl. Phys. 102:063510

[31] Gustavsen RL, Sheffield SA, Alcon RR and Hill LG (1998) Shock Initiation of New and Aged PBX 9501 Measured with Embedded Electromagnetic Particle Velocity Gauges LA-13634-MS Los Alamos National Laboratory Los Alamos, NM

[32] Dick JJ, Forest CA, Ramsay JB and Seitz WL (1988) The Hugoniot and shock sensitivity of a plastic□bonded TATB explosive PBX 9502. J. Appl. Phys. 63:4881-4888

[33] Dobratz BM and Crawford PC (1985) LLNL Explosives Handbook. Properties of chemical explosives and explosive simulants UCRL-82997 Lawrence Livermore National Laboratory Springfield, VA

[34] Stevens LL and Eckhardt CJ (2005) The elastic constants and related properties of beta-HMX determined by Brillouin scattering. J. Chem. Phys. 122:174701

[35] Millett JCF, Bourne NK and Gray GT (2004) The shock induced equation of state of a fluorinated trimer. J. Appl. Phys. 96:5500-5504

[37] Bourne NK and Gray GT (2005) Dynamic response of binders; Teflon, Estane and Kel-F-800. J. Appl. Phys. 98:123505

[38] Bourne NK (2003) A 50 mm bore gun for dynamic loading of materials and structures. Meas. Sci. Technol. 14:273-278

[39] Rosenberg Z, Bourne NK and Millett JCF (2007) On the effect of manganin gauge geometries upon their response to lateral stress. Meas. Sci. Technol. 18:1843-1847

[40] Rosenberg Z, Yaziv D and Partom Y (1980) Calibration of foil-like manganin gauges in planar shock wave experiments. J. Appl. Phys. 51:3702-3705

[41] Millett JCF, Lowe MR, Appleby-Thomas G and Roberts A (2015) The mechanical and optical response of polychlorotrifluoroethylene to one-dimensional shock loading. Met. Mat. Trans. A 47A:697-705

[42] Sheffield SA, Gustavsen RL and Alcon RR (1998) Porous HMX intitation studies_ Sugar as an inert simulant. In: S. C. Schmidt, D. P. Dandekar and J. W. Forbes (ed) Shock Compression of Condensed Matter - 1997. AIP Press, Melville, NY, pp 575-578

[43] Millett JCF, Bourne NK and Rosenberg Z (1996) Shear stress measurements in copper, iron and mild steel under shock loading conditions. In: (ed) Shock Compression of Condensed Matter 1995. American Institute of Physics, Melville, NY, pp 515-518

[44] Millett JCF, Whiteman G, Park NT, Case S and Bourne NK (2013) The role of cold work on the shock response of tantalum. J. Appl. Phys. 113:233502

[45] Rosenberg Z, Brar NS and Bless SJ (1991) Dynamic high-pressure properties of AlN ceramic as determined by flyer plate impact. J. Appl. Phys. 70:167-171

[46] Bourne NK (2008) The relation of failure under 1D shock to the ballistic performance of brittle materials. Int. J. Imp. Engng. 35:674-683

[47] Millett JCF, Bourne NK and Barnes NR (2002) The behaviour of an epoxy resin under one-dimensional shock loading. J. Appl. Phys. 92:6590-6594

[48] Jordan JL, Casem D and Zellner M (2016) Shock response of polymethylmethacrylate. J. Dynamic Behavior Mater. 22:372-378

[49] Petel OE and Higgins AJ (2010) Shock wave propagation in dense particle suspensions. J. Appl. Phys. 108:114918